

RESEARCH

Open Access



# Computational modeling and ligand-based design of some novel hypothetical compound as prominent inhibitors against *Mycobacterium tuberculosis*

Shola Elijah Adeniji<sup>1\*</sup>  and Olajumoke Bosede Adalumo<sup>2</sup>

## Abstract

**Background:** Time consumed and expenses in discovering and synthesizing new hypothetical drugs with improved biological activity have been a major challenge toward the treatment of multi-drug-resistant strain *Mycobacterium tuberculosis* (TB). To solve the above problem, quantitative structure activity relationship (QSAR) is a recent approach developed to discover novel agents with better biological activity against *M. tuberculosis*.

**Results:** A validated QSAR model was developed in this study to predict the biological activities of some anti-tubercular compounds and to design new hypothetical drugs is influenced with the molecular descriptors, AATS7s, VR1\_Dzi, VR1\_Dzs, SpMin7\_Bhe, and TDB8e, which has been validated through internal and external validation test. Prior to high anti-tubercular activity of the lead compound, compound 17 served as a template structure to design compounds with improved activity. Among the compounds designed, compounds 17i, 17j, and 17n were observed with improved anti-tubercular activities which ranges from 8.8981 to 9.0377 pBA.

**Conclusion:** The outcome of this research is recommended for pharmaceutical and medicinal chemists to synthesis and carry out an in vivo and in vitro screening for the proposed designed compounds in order to substantiate the computational findings.

**Keywords:** Model, Quinoline, QSAR, Tuberculosis

## Background

Multi-drug resistance strain (TB) has posed a challenge toward the treatment of tuberculosis in the global community. World Health Organization in (2018) has reported 9.0 million people infected with tuberculosis, 360,000 HIV patients who were living with tuberculosis, death of 230,000 children, and death of 1.6 million people worldwide [1]. Some of the notable commercially sold drugs administered to people infected with tuberculosis are isoniazid (INH), pyrazinamide (PZA), rifampicin (RMP), and para-amino salicylic acid (PAS). The emergence of multi drug-resistant strains of

*M. tuberculosis* toward the aforementioned drugs has led to advances in searching for new and better approach that is precise and fast in developing a novel compound with improved biological activity against *M. tuberculosis*.

The advance of computational chemistry has led to development of new drug. Computational methods which reduced the cost for effective evaluation of large virtual database of chemical compounds are currently employed in designing new drugs. Such method includes complex network theory, quantitative structure–activity relationships (QSAR) models, Machine Learning (ML), and Artificial Neural Networks (ANN) analysis. For the time being, QSAR is a theoretical approach with widely used computational method in predicting and designing new hypothetical drug candidate [2]. The application of QSAR

\* Correspondence: [shola4343@gmail.com](mailto:shola4343@gmail.com)

<sup>1</sup>Chemistry department, Ahmadu Bello University, Zaria, Nigeria Kaduna State 810107, Nigeria

Full list of author information is available at the end of the article

technique to this problem has a potential to minimize the effort and time required to discover new compounds or to improve current compounds in terms of their efficiency. Multi variant QSAR model is expressed mathematically to relate the physical, chemical, biological, or environmental activities of interest with measurable or computable parameters such as physicochemical, topological, stereochemical, or electronic indices called molecular descriptors. Meanwhile, some prominent researchers [3–6] have successfully established QSAR models to show the relationship between some derivatives such as triazole, chalcone, quinolone, 7-methyljuglone, pyrrole, and their respective biological activities using the QSAR approach. Hence, this research was aimed to build a robust QSAR model with high predictability and to design new potent hypothetical compounds with proposed better anti-tubercular activity.

## Methods

### Data collection

The molecules of derivatives of 2,4-disubstituted quinoline derivatives reported as anti-*Mycobacterium tuberculosis* which were used in this study were obtained from the literature [7]. The list of these compounds and their biological activities were presented in Table 1.

### Biological activities

The biological activities of 2,4-disubstituted quinoline derivatives as potent anti-tubercular agents were initially expressed in percentage (%) and then converted to logarithm unit using Eq. 1 below in order to increase the linearity and approach normal distribution of the activity values. The observed structures and the biological activities of these compounds were presented in Table 1 [4].

$$\left[ \text{pBA} = \log \left( \frac{\text{molecular weight}_{(\text{g/mol})}}{\text{Dose}_{(\text{g/mol})}} \right) \left( \frac{\text{percentage } (\%)}{100 - \text{percentage } (\%)} \right) \right] \quad (1)$$

### Molecular optimization

The Spartan 14 software version 1.1.4 was used to optimize all the inhibitory compounds in order for the compounds to attain stable conformation at a minimal energy. The strain energy from the molecules was removed by employing molecular mechanics force field (MMFF), and complete optimization was achieved with the aid of density functional theory (DFT) by utilizing the (B3LYP) basic set [4].

### Generation of molecular descriptor

A descriptor is a mathematical logic that defines the properties of a molecule in a numeral term based on the connection between the biological activity of each molecule and its molecular structure. Descriptors for all the

**Table 1** Geometrical structures of inhibitory compounds as anti-tubercular agents

No.	Molecular structure	R1	TPSA	TPSA <sub>max</sub>	TPSA <sub>min</sub>	TPSA <sub>avg</sub>
1						

inhibitory molecules were calculated with the aid of the PaDEL descriptor software version 2.20, and a total of 1879 molecular descriptors were generated.

#### Normalization and pretreatment of data

For each of the variable (descriptor) to have the same chance at the inception so as to influence the QSAR model, the descriptor values generated from the PaDEL descriptor software version 2.20 were subjected to normalization using Eq. 2 [8].

$$D = \frac{d_1 - d_{\min}}{d_{\max} - d_{\min}} \quad (2)$$

where  $d_{\max}$  and  $d_{\min}$  are the maximum and minimum value for each descriptor column of  $D$ .  $d_1$  is the descriptor value for each of the molecule. Immediately after the data have been normalized, the normalized data were then subjected to pre-treatment so as to remove redundant descriptors.

#### Generation training and test set

The whole compounds that made up the data set were divided into training and test set in proportion of 70 to 30% using Kennard and Stone's algorithm which was incorporated in DTC lab software. The development of the QSAR model and internal validation test were performed on the training set while the confirmation of the developed model was performed on test set.

#### Building of QSAR models and internal validation test

The QSAR models were built by adopting the Genetic Function Approximation (GFA) technique incorporated in the Material Studio software version 8.0 to select the optimum descriptors for the training set. Meanwhile, multi-linear regression approach (MLR) was used as a modeling tool to develop the multi-variant equations by placing the activity data in the last column of Microsoft Excel 2013 spread sheet which was later imported into the Material Studio software version 8.0 to generate the QSAR model. The internal validation test to affirm the built model is robust and also has a high predictability that was also performed in the Material Studio software version 8.0 and reported.

#### Evaluation of leverage values (applicability domain)

Influential and outlier molecule present in both the training and test set were determined by employing the applicability domain approach. The leverage  $h_i$  approach as defined in Eq. 3 was used to define applicability domain space  $\pm 3$  for outlier molecule [9].

$$h_i = M_i (M^T M)^{-1} M_i^T \quad (3)$$

where  $M_i$  represents the matrix of  $i$  for the training set.  $M$  represents the  $n \times d$  descriptor matrix for the

training set, and  $M^T$  is the transpose of the training set ( $M$ ).  $M_i^T$  represents the transpose matrix  $M_i$ . Meanwhile, the warning leverage  $h^*$  defined in Eq. 4 is the limit boundary to check for an influential molecule.

$$h^* = 3 \frac{(d + 1)}{N} \quad (4)$$

where  $d$  is the total number of descriptors present in the built model, and  $N$  is the total number of compounds that made up the training set.

#### Y-randomization validation test

Y-randomization test is one of the external validation criteria which has to be considered in order to ascertain that the developed model is not built by chance [10]. Random shuffling of the data was performed on the training set following the principle laid by [11]. The activity data (dependent variable) were shuffled while the descriptors (independent variables) were kept unchanged in order to generate the multi-linear regression (MLR) model. For the developed QSAR to pass the Y-randomization test, the  $R^2$  and  $Q^2$  values for the model must be significantly low for numbers of trials while Y-randomization coefficient ( $cR_p^2$ ) shown in Eq. 5 must be  $\geq 0.5$  in order to establish the robustness of the model.

$$cR_p^2 = R \times [R^2 - (R_r)^2]^2 \quad (5)$$

where  $cR_p^2$  is the Y-randomization coefficient,  $R$  is the correlation coefficient, and  $R_r$  is the average "R" of random models.

#### Affirmation of the build model

The internal and external validation criteria for both test and training set reported were compared with the generally accepted threshold value shown in Table 6 for any QSAR model [9–12] in order to affirm the reliability, fitting, stability, robustness, and predictability of the developed models.

## Results

### Model 1

pBA =  $-7.836545646 \times \text{AATS7s} + 0.201962934 \times \text{VR1\_Dzi} + 0.087893211 \times \text{VR1\_Dzs} - 4.204663658 \times \text{SpMin7\_Bhe} + 0.674915710 \times \text{TDB8e} + 29.11653208$

### Model 2

pBA =  $-4.790218643 \times \text{AATS5e} + 0.082643756 \times \text{VR3\_Dzv} - 3.953009651 \times \text{SpMin7\_Bhe} + 0.094784839 \times \text{TDB7e} + 0.024520722 \times \text{RDF90i} + 41.534742802$

EE is the standard error of estimation,  $w$  is the total number of terms present in the built model except the constant term,  $j$  is the number of descriptors confined in

the built model,  $q$  is a user-defined factor, and  $N$  is the number of compounds of training set.  $Y_{\text{obs}}$ ,  $\bar{Y}_{\text{training}}$ , and  $Y_{\text{pred}}$  are the observed activity, mean observed activity of the training compounds and the predicted activity respectively.  $r^2$  is correlation coefficients of the plot of observed activity against predicted activity values,  $r_o^2$  is the correlation coefficients of the plot of observed activity against predicted activity values at zero intercept,  $r_o'^2$  is the correlation coefficients of the plot of predicted activity against observed activity at zero intercept [7, 9, 10].

## Discussion on designed compounds

### Discussion

#### QSAR studies

Optimum QSAR model for predicting the derivatives of 2,4-disubstituted quinoline against *M. tuberculosis* was successfully achieved by adopting the combination of computational and theoretical method. Data set comprises of 36 compounds was partitioned into 25 training set and 11 test set using Kennard and Stone algorithm method. The 25 training set compounds were used to derive QSAR model using the multi-linear regression technique which also served as data set for internal validation test while the external validation test for the derived model was conducted on the test set.

The observed activities reported in literature, the calculated activities calculated for all the anti-tubercular compounds, the leverage values, and the residual values were presented in Table 1. The difference between the observed activities and calculated activities is the residual values which were observed to be significant low [13–15]. The low residual value indicates that the model built has a good predictive ability.

The optimum (2D and 3D) descriptors that efficiently describe the anti-tubercular compounds in relation to their biological activities were selected by the GFA approach. The characterization and relative information on the molecular structure of the anti-tubercular agent illustrated by the descriptors were reported in numerical value as shown in Table 2.

Various statistical analyses were conducted on the calculated descriptors in order to check the validity of the built model as reported in Table 3. Variance inflation

**Table 2** Descriptors name and class in model 1

S/ NO	Name of descriptor(s)	Descriptor symbols	Class
1	Average Broto-Moreau autocorrelation-lag 7/weighted by I-state	AATS7s	2D
2	Randic-like eigenvector-based index from Barysz matrix/weighted by first ionization potential	VR1_Dzi	2D
3	Randic-like eigenvector-based index from Barysz matrix/weighted by I-state	VR1_Dzs	2D
4	Smallest absolute eigenvalue of Burden modified matrix-n 7/weighted by relative Sanderson electronegativities	SpMin7_Bhe	2D
5	Topological distance based autocorrelation-lag 8/weighted by Sanderson electronegativities	TDB8e	3D

factor (VIF) was evaluated for all the descriptors in order to determine the degree of correlation between each the descriptor. Generally, VIF value equals to 1 or falls with 1 and 5 signify non-existence of inter-correlation among the descriptors. However, if the VIF value is greater than 10, it signify that the model developed is unstable, hence the model should be re-checked if necessary. Regarding the VIF values for each of the descriptors which were found to be less than 5 as reported in Table 3 affirm that the descriptors were significantly orthogonal to each order since there is no inter-correlation between them. The degree of contribution that each descriptor plays in the built model was evaluated by determining the standard regression coefficient ( $b_j^s$ ) and mean effect (ME). The magnitude and signs for  $b_j^s$  and ME values reported in Table 4 indicate strength and direction with which each descriptor influence the activity model. The relationship between the descriptors and biological activity of each compound was determined by one way analysis of variance (ANOVA). The probability value of each of the descriptor at 95% confidence level was found to be ( $p < 0.05$ ) as presented in Table 3. Therefore, this signify that the alternative hypothesis that says there is a direct relationship between the biological activity of each compound and the descriptor swaying the built model is accepted; thus, null hypothesis proposing no direct relationship between biological activity of each compound and the descriptor swaying the built model is rejected. To further justify the validation of the

**Table 3** Statistical analysis and validation of descriptors model 1

Descriptor	Standard regression coefficient ( $b_j$ )	Mean effect (ME)	P value (confidence interval)	VIF	Standard error
AATS7s	− 0.2854	− 0.2651	2.23E-04	3.0925	5.11E-05
VR1_Dzi	0.4312	0.4176	0.00719	1.6328	2.98E-06
VR1_Dzs	0.1729	0.1623	4.34E-04	2.7301	4.78E-05
SpMin7_Bhe	− 0.4287	− 0.4017	3.42E-04	3.2001	3.09E-04
TDB8e	0.6341	− 0.6287	2.84E-05	1.0034	0.4302

**Table 4** Coefficient of Pearson's correlation for descriptor in model

Inter-correlation					
	AATS7s	VR1_Dzi	VR1_Dzs	SpMin7_Bhe	TDB8e
AATS7s	1				
VR1_Dzi	0.4318	1			
VR1_Dzs	0.5324	0.4091	1		
SpMin7_Bhe	0.3912	- 0.0123	- 0.0291	1	
TDB8e	0.1008	- 0.0189	0.0183	0.0298	1

descriptors in the activity model, Pearson's correlation statistic was conducted to also check whether there is inter-correlation between each descriptor. The correlation coefficient between each descriptors reported in

Table 4 was all  $< \pm 0.8$ . Hence, this implies that all the descriptors were void of multicollinearity.

Validation results for both the external and internal assessment to assure that the built models are reliable and robust were presented in Table 5. These results were all in full agreement with the general validation criteria presented in Table 5 to truly indorse that the stability and robustness of the model is valid. Reference to these validation results obtained, model one was selected and established to be the prime model which was used to predict the biological activities of 2, 4-disubstituted quinoline against *M. tuberculosis*.

The built QSAR model and results obtained in this research were compared with recent model developed in the literature [3, 6] as shown below:

**Table 5** Internal and external validation parameters for each model

S/NO	Validation parameters	Formula	Threshold	Model 1	Model 2
Internal validation					
1	Friedman's lack of fit (LOF)	$\frac{SEE}{(1 - \frac{w+qx}{N})^2}$		0.0274	0.0301
2	R-squared	$1 - \left[ \frac{\sum (Y_{obs} - Y_{pred})^2}{\sum (Y_{obs} - \bar{Y}_{training})^2} \right]$	$R^2 > 0.6$	0.9183	0.8429
3	Adjusted R-squared	$\frac{R^2 - P(N-1)}{N - P + 1}$	$R^2_{adj} > 0.6$	0.8854	0.8189
4	Cross validated R-squared ( $Q^2_{cv}$ )	$1 - \left[ \frac{\sum (Y_{pred} - Y_{obs})^2}{\sum (Y_{obs} - \bar{Y}_{training})^2} \right]$	$Q^2 > 0.6$	0.8202	0.7400
5	Significant regression			Yes	Yes
6	Critical SOR <i>F</i> value (95%)	$\frac{\sum (Y_{pred} - Y_{obs})^2}{p} / \frac{\sum (Y_{pred} - Y_{obs})^2}{N - p - 1}$	$F_{(test)} > 2.09$	4.3892	4.3892
7	Replicate points			0	0
8	Computed observed error			0	0
9	Min expt. error for non-significant LOF (95%)			0.0278	0.0278
Model randomization					
10	Average of the correlation coefficient for randomized data ( $\bar{R}_r$ )		$\bar{R} < 0.5$	0.3371	0.3983
11	Average of determination coefficient for randomized data ( $\bar{R}_r^2$ )		$\bar{R}_r^2 < 0.5$	0.1521	0.1763
12	Average of leave-one-out cross-validated determination coefficient for randomized data ( $\bar{Q}_r^2$ )		$\bar{Q}_r^2 < 0.5$	- 1.3198	- 1.3719
13	Y-randomization coefficient ( $cR_p^2$ )	$R^2 \times (1 - \sqrt{ R^2 - \bar{R}_r^2 })$	$cR_p^2 > 0.6$	0.7362	0.7058
External validation					
14	Slope of the plot of observed activity against predicted activity values at zero intercept ( <b>k</b> )	$\frac{\Delta Y_{obs}}{\Delta Y_{pred}}$	$0.85 < k < 1.15$	1.0013	1.0582
15	Slope of the plot of predicted against observed activity at zero intercept ( <b>k'</b> )	$\frac{\Delta Y_{pred}}{\Delta Y_{obs}}$	$0.85 < k < 1.15$	0.9290	0.9016
16	$ r_0^2 - r_0'^2 $		$< 0.3$	0.0834	0.0610
17	$\frac{r^2 - r_0^2}{r^2}$		$< 0.1$	0.0028	0.0042
18	$\frac{r^2 - r_0'^2}{r^2}$		$< 0.1$	0.0610	0.0582
19	$R^2_{test}$	$R^2_{test} = 1 - \frac{\sum (Y_{pred_{test}} - Y_{obs_{test}})^2}{\sum (Y_{pred_{test}} - \bar{Y}_{training})^2}$	$> 0.6$	0.8052	0.7281



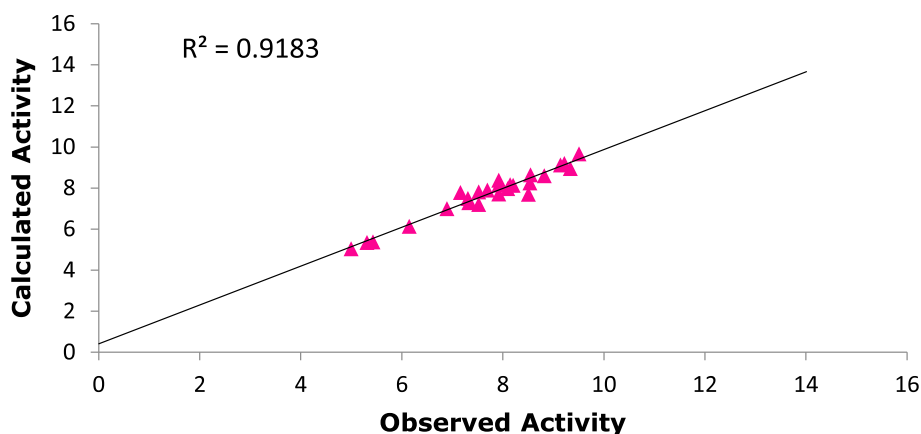


**Fig. 1** Plot of predicted activity against observed activity of training set

$\text{pBA} = -0.307001458(\text{MATS2s}) + 1.528715398(\text{nHBint3}) + 3.976720227(\text{maxtsC}) + 0.016199645(\text{TDB9e}) + 0.089381479(\text{RDF90i}) - 0.107407822(\text{RDF110s}) + 4.057082751$ ,  $R^2 = 0.92024$ ,  $R_{\text{adj}} = 0.9102$ ,  $Q_{\text{cv}}^2 = 0.8954$ , and  $R^2_{\text{pred}} = 0.8842$  [3]

$\text{pIC50} = -2.040810634(\text{nCl}) - 19.024890361(\text{MATS2m}) + 1.855704759(\text{RDF140s}) + 6.739013671$ ,  $R^2 = 0.9480$ ,  $R_{\text{adj}} = 0.9350$ ,  $Q_{\text{cv}}^2 = 0.8799$ , and  $R^2_{\text{pred}} = 0.7690$  [6]

The validation factors reported in this work and those reported in the literature were all in agreement with the validation parameters presented in Table 5 which really inveterate that the model generated is predictive and robust.

The coefficient of Y-randomization ( $cR_p^2$ ) with significant value of 0.7362 greater than threshold value of 0.5 reported in Table 5 provides a reasonable support that the model built is robust and not just by chance.

The graphical representation to show the degree of correlation between the calculated activities and

observed activities of the training and test set were shown in Figs. 1 and 2. The correlation coefficient ( $R^2$ ) value of 0.9183 and 0.8052 for both the training set and test set shows that there is a high correlation existing between the calculated activities and observed activities of the training and test set which were also in agreement with the accepted QSAR threshold values reported in Table 6.

The residual plot shown in Fig. 3 signify that there is no indication of computational incompetency and inaccuracy in the QSAR model derived as all the standard residual values for both training and test set were found within the defined boundary of  $\pm 2$  on the standard residual activity axis.

The Williams plot to show the applicability domain space (AD) is shown in Fig. 4. However, compound (number 30) is found to have a leverage value greater than the predicted warning leverage ( $h^* = 0.60$ ). Therefore, it can be infer that compound (number 30) is an influential molecule. Moreover, it is also

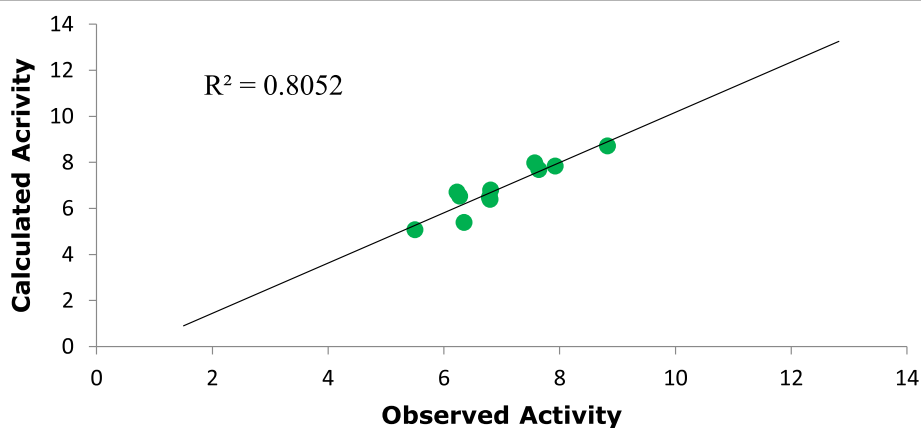


**Fig. 2** Plot of predicted activity against observed activity of test set

**Table 6** Binding affinity, hydrogen bond, and hydrophobic interaction of the ligands (2,4-disubstituted quinolone derivatives) with *M. tuberculosis* target (DNA gyrase)

Ligand	Binding affinity (BA) Kcal/mol	Target	Hydrogen bond		Hydrophobic interaction
			Amino acid	Bond length (Å)	
1	– 7.2	DNA gyrase	PRO124	2.251	VAL278, TRP103, HIS220, GLN277
2	– 7.5	DNA gyrase	ARG98	2.9399	GLN277, PRO285, HIS220, VAL78
3	– 7.7	DNA gyrase	ASP94 TRP182	2.3878	PRO124, VAL138, GLN101, CYS112
4	– 7.7	DNA gyrase	ARG98	1.4999	PRO124, VAL97, HIS220
5	– 7.9	DNA gyrase	ASP94	2.1801	VAL278, PRO119, GLN101, ASP122
6	– 8.3	DNA gyrase	SER102	2.529	ASP122, ALA167, TRP182, SER247
7	– 8.2	DNA gyrase	ARG98 GLY120 SER118	4.287 2.6231, 2.8491 2.6198	TYR276, ASP94, VAL97, PRO124
8	– 8.8	DNA gyrase	HIS220	2.4765	PHE228, ALA173, PRO119, TRP182, SER247
9	– 8.4	DNA gyrase	LEU213 ARG184	1.461	MET99, VAL78, TRP182, SER118, ASP122,
10	– 8.2	DNA gyrase	PRO119 GLY120	2.1738	VAL77, SER247, ARG98, ASP94, VAL182
11	– 9.7	DNA gyrase	ASP94 TRP103	1.383	GLY120, GLY120, SER118, PHE168, PRO285, VAL78,
12	– 8.6	DNA gyrase	SER104 VAL77	2.023	TRP162, CYS145, ASP122, VAL78, PRO126, ARG98,
13	– 8.1	DNA gyrase	PRO	2.221	PRO34, PRO285, PHE177, VAL27, MET99
14	– 8.4	DNA gyrase	VAL169 ARG134 PRO285	2.6021	MET99, ASP122, PHE232
15	– 9.1	DNA gyrase	GLY145 SER205	2.4909	VAL98, ALA223, MET145, MET99, LEU164
16	– 8.1	DNA gyrase	ARG98 SER118 GLY120	3.3701 2.8704 1.9128, 3.2821	PRO124, VAL97, VAL97, ASP94, PRO123, ASP122,
17	– 18.8	DNA gyrase	ARG98	1.99395	CYS174, ALA67, ASN74, GLY120, MET99,
18	– 9.1	DNA gyrase	LEU114 ALA78	2.3983	LEU164, VAL228, PHE168, GLY232, TYR276
19	– 9.7	DNA gyrase	ALA167 ARG94	1.3965	ALA233, LYS136, MET99, VAL228
20	– 11.6	DNA gyrase	MET99	2.3975	TRP142, PHE88, PRO169, VAL78, LEU 156
21	– 9.9	DNA gyrase	GLN223 TYR276	2.5093	ARG98, LEU103, ALA167, PHE168, MET234,
22	– 6.8	DNA gyrase	PHE212 TRP182	1.8408	VAL78, LEU123, SER119, ALA233, TYR276,
23	– 10.7	DNA gyrase	LSY146 TRP143	2.1665	PHE168, CYS254, TRP182, ALA167, VAL78, VAL82
24	– 7.9	DNA gyrase	ARG98 CYS156	1.5984	ALA167, LEU 103, TRP112, ARG386
25	– 7.1	DNA gyrase	TRP182	2.3663	ARG72, ALA143, VAL78, GLN154
26	– 8	DNA gyrase	PHE256 ARG143	1.287	TRP182, CYS345, ALA176, PHE 168,
27	– 9.2	DNA gyrase	–	–	PRO285, MET 232, SER108, ALA137
28	– 8.5	DNA gyrase	–	–	LEU164, VAL178, PRO169, PHE98, VAL228,
29	– 8.1	DNA gyrase	ARG145	1.9217	LEU234, VAL228, CYS 144, ALA233, VAL78
30	– 8.2	DNA gyrase	TRP182 MET99	2.3896	PRO34, PRO94, PHE93, VAL178, PHE241, PRO169

**Table 6** Binding affinity, hydrogen bond, and hydrophobic interaction of the ligands (2,4-disubstituted quinolone derivatives) with *M. tuberculosis* target (DNA gyrase) (Continued)

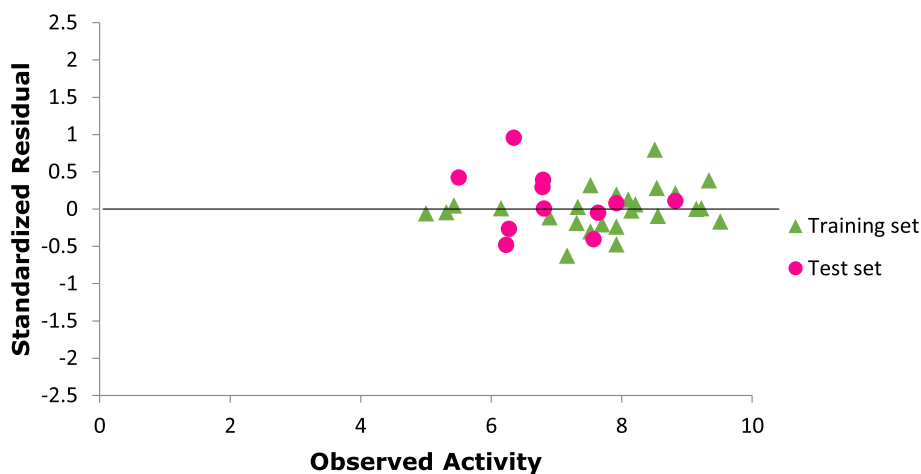
Ligand	Binding affinity (BA) Kcal/mol	Target	Hydrogen bond		Hydrophobic interaction
			Amino acid	Bond length (Å)	
31	− 9.3	DNA gyrase	ARG98	1.3896	PHE168, ALA137, TRP182, VAL122, PHE220
32	− 11.4	DNA gyrase	TYR276	3.1345	VAL78, HIS220
33	− 7.1	DNA gyrase	GLN277	2.5007	PHE338, ALA233, TYR276, ASP122, CYS345
34	− 9.6	DNA gyrase	HIS220 SER104 MET99	3.2896	PHE285, GLY120, SER118
35	− 9.4	DNA gyrase	TYR276	2.5007	TRP182, PHE168, TRP182, ALA167, TYR276
36	− 8.2	DNA gyrase	ALA167 LEU137	1.3907	VAL167, CYS234, ARG165, ARG98, GLN385, TYR276, GLN385
Ethambutol	− 5.8	DNA gyrase	ALA337	2.59739	–
Isoniazid	− 14.6	DNA gyrase	SER279 ALA337	2.29943 2.52954, 2.24657	CYS345, PHE338

observed that all the compounds fall within the defined space of  $\pm 3$  which indicates that no compound is said to be outlier.

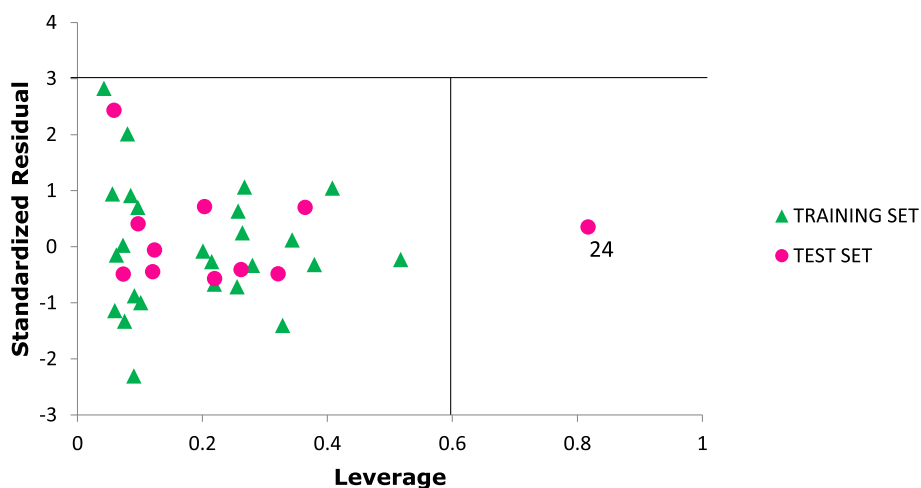
#### In silico design for new derivatives based on Lead compound 17

Ligand-based approach was employed to design new compounds with better anti-tubercular activities via modification of the template by deletion, insertion, and substitution of active substituent(s) into the template structure. The choice of template used in this study was (E)-N-benzyl-2-(2-benzylidenehydrazinyl)-quinoline-4-carboxamide (i.e., molecule 17 in Table 1) due to its relative high anti-tubercular activity which also falls within the model applicability domain (AD) space shown in Fig. 4. The modification was easily

made around N-ethylacetamide and 2-methylhydrazine moiety of the template at positions 16 and 23 shown in Fig. 5. The QSAR model built indicated that increase in the values of descriptors, VR3\_Dzp, VR1\_Dzi, and VR1\_Dzs and influences the activity positively. This implies that increase in the value of these descriptors also augment the values of the activity in the same direction. Variation of the substituent at positions 16 and 23 of the template structure with alkyl group, benzene derivatives, and substituted alkyl amines lead to generation of fourteen compounds with better anti-tubercular activities reported in Table 7. The leverage values predicted for the designed compounds were used to screen and confirm whether these compounds were within their model AD. Based on the leverage value predicted for each compound in

**Fig. 3** Plot of standardized residual activity versus observed activity





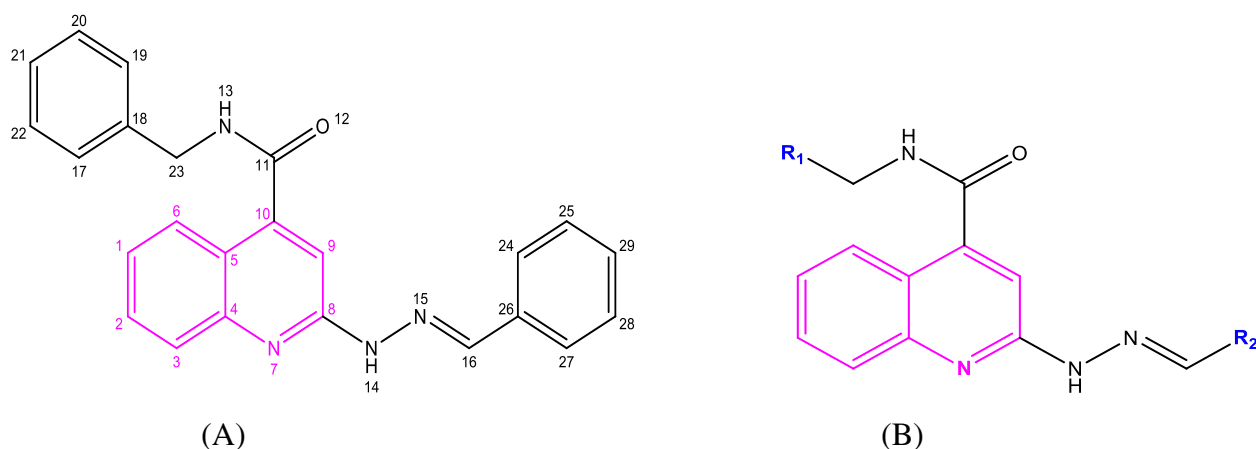
**Fig. 4** The Williams plot of the standardized residuals versus the leverage value

Table 7 assured that each compound have a low leverage value compared with the warning leverage  $h^* = 0.64$  shown in Fig. 5. Hence, this signified that all the designed compounds fall within their model AD space. Among the compounds designed, compounds 17i, 17j, and 17n were observed with better anti-tubercular activities. This was as a result of substitution at positions 16 and 23 of the template structure with N-substituted alkyl amine which act as electron releasing group via positive inductive effect (+I). Due to the positive +I effect of the alkyl group attached to the template structure, the nitrogen becomes strongly electronegative, so the lone pair of electron on N-atom is easily available. The steric hindrance of the bulky alkyl group ( $3^0$  amine) observed in the compound 17j accounts for the decrease in its reactivity when compared to compound 17i ( $1^0$  amine) and 17n

( $2^0$  amine). Based on the decreasing order of amine,  $(\text{CH}_3)_2\text{NH} > \text{CH}_3\text{NH}_2 > (\text{CH}_3)_3\text{N} > \text{NH}_3$ , suggests why compound 17n was observed with prominent activity.

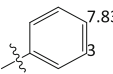
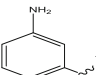
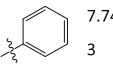
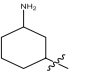
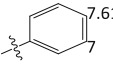
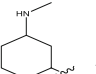
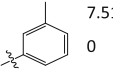
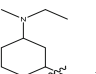
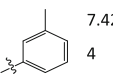
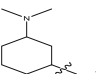
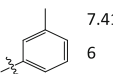
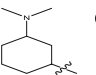
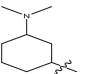
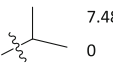
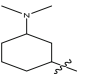
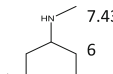
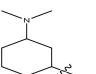
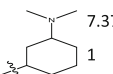
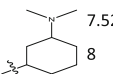
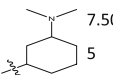
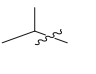
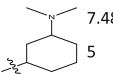
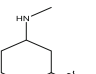
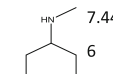
### Conclusion

This work addresses the quantitative structure activity relationship (QSAR) between quinoline derivatives and their biological activities against *Mycobacterium tuberculosis*. The QSAR model was established to predict the reported experimental activities of 2,4-disubstituted quinoline derivatives against *M. tuberculosis* via computational modeling approach under the influence of optimum descriptors: AATS7s, VR1\_Dzi, VR1\_Dzs, SpMin7\_Bhe, and TDB8e. The lead compound (compound 17) with higher anti-tubercular activity was used as a structural template to designed new hypothetical drug candidates. Among the



**Fig. 5** a Shows the lead compound (17) for 2,4-disubstituted quinoline. b Shows the general formula of the lead compound (17) for 2,4-disubstituted quinoline as a design template

**Table 7** Designed molecule, predicted descriptors, and calculated activities for template 17 of 2,4-quiloline derivative

Compound ID	R <sub>1</sub>	R <sub>2</sub>	AATS 5e	VR3_D zp	VR1_D zi	VR1_D zs	SpMin7_ Bhe	Predicted Activity (pBA)	Leverage
17a	CH <sub>3</sub>		7.839 3	17.429 1	451.48 56	418.73 31	0.6986	8.2004	0.1327
17b			7.743 3	19.261 9	512.23 93	463.40 70	0.8252	8.2614	0.3711
17c			7.617 3	19.672 3	532.40 54	477.50 32	0.9564	8.3264	0.4193
17d			7.516 0	26.591 2	577.81 45	604.65 24	1.1100	8.5258	0.2586
17e			7.428 4	25.823 5	623.03 29	687.69 10	1.1891	8.6570	0.2674
17f			7.416 6	25.047 5	638.78 21	637.42 93	1.1966	8.6670	0.3510
17g		CH <sub>3</sub>	7.439 0	14.500 8	257.17 67	246.88 07	1.0736	7.9161	0.4394
17h			7.480 0	24.753 3	583.47 23	501.81 11	1.1357	8.4934	0.3877
17i			7.430 6	27.626 7	877.38 99	686.65 16	1.2192	9.0377	0.2115
17j			7.375 1	26.656 0	770.48 40	650.33 87	1.2577	8.8981	0.3711
17k	CH <sub>3</sub>		7.520 8	20.229 1	550.27 84	466.01 25	1.0563	8.3986	0.4542
17l	CH <sub>3</sub> CH <sub>2</sub>		7.503 5	23.096 1	562.85 84	490.70 80	1.1001	8.4280	0.0906
17m			7.487 5	26.505 1	569.84 85	496.54 43	1.1467	8.4484	0.2126
17n			7.440 6	29.626 7	977.38 99	746.65 16	1.2324	9.2007	0.0332

compounds designed, compounds 17i, 17j, and 17n were observed with improved anti-tubercular activities which ranges from 8.8981 to 9.0377 pBA. The outcome of this research is recommended for pharmaceutical and medicinal chemists to synthesis and carry out an in vivo and in vitro screening for the proposed designed compounds in order to substantiate the computational findings.

#### Acknowledgements

None

#### Authors' contributions

SE and OB did the conception and design of the work. SE and OB did the acquisition and analysis of the data. SE interpreted the data. SE drafted the manuscript. SE and OB substantially revised the manuscript. All authors read and approved the final manuscript.

#### Funding

None

#### Availability of data and materials

It has been reported and cited in the methodology part of the manuscript.

#### Ethics approval and consent to participate

Not applicable for that section

#### Consent for publication

Not applicable for that section

#### Competing interests

Not applicable for that section

#### Author details

<sup>1</sup>Chemistry department, Ahmadu Bello University, Zaria, Nigeria Kaduna State 810107, Nigeria. <sup>2</sup>Department of Science Education, Ajasin University, Akungba Akoko, Ondo, State 342211, Nigeria.

Received: 17 December 2019 Accepted: 8 April 2020

Published online: 25 May 2020

#### References

1. W.H.O (2018) <http://www.who.int/news-room/fact-sheets/detail/tuberculosis>
2. Hansch C, Kurup A, Garg R, Gao H (2001) Chem-bioinformatics and QSAR: a review of QSAR lacking positive hydrophobic terms. *Chem Rev* 101:619–672
3. Ogadimma AI, Adamu U (2016) Analysis of selected chalcone derivatives as *Mycobacterium tuberculosis* inhibitors. *Open Access Library J* 3:1–13
4. Adeniji SE, Uba S, Uzairu A (2018) QSAR Modeling and molecular docking analysis of some active compounds against *Mycobacterium tuberculosis* receptor (Mtb CYP121). *J Pathog* 2018
5. Adeniji SE, Uba S, Uzairu A (2018) A Novel QSAR Model for the evaluation and prediction of (E)-N'-Benzylideneisonicotinohydrazide derivatives as the potent anti-mycobacterium tuberculosis antibodies using genetic function approach. *Phys Chem Res* 6:479–492
6. Adeniji SE, Uba S, Uzairu A (2019) A derived QSAR model for predicting some compounds as potent antagonist against *M. tuberculosis*: a theoretical approach. *Hindawi Adv Prev Med*:5173786
7. Nayyar A, Jain R (2008) Synthesis and anti-tuberculosis activity of 2, 4-disubstituted quinolines. *Ind J Chemist Sect B Org Med Chem* 47:117–128
8. Singh P (2013) Quantitative structure-activity relationship study of substituted-[1, 2, 4] oxadiazoles as S1P1 agonists. *J Curr Chem Pharm Sci* 3: 64–79
9. Veerasamy R, Rajak H, Jain A, Sivadasan S, Varghese CP, Agrawal RK (2011) Validation of QSAR models-strategies and importance. *Int J Drug Des Discov* 3:511–519
10. Tropsha A, Gramatica P, Gombar VK (2003) The importance of being earnest: validation is the absolute essential for successful application and interpretation of QSPR models. *Mol Inform* 22:69–77
11. Adeniji SE, Uba S, Uzairu A (2018) Theoretical modeling and molecular docking simulation for investigating and evaluating some active

compounds as potent anti-tubercular agents against MTB CYP121 receptor. *Future J Pharm Sci* 4:284–295

12. Roy K, Chakraborty P, Mitra I, Ojha PK, Kar S, Das RN (2013) Some case studies on application of "rm2" metrics for judging quality of quantitative structure-activity relationship predictions: emphasis on scaling of response data. *J Comput Chem* 34:1071–1082
13. Ibrahim MT, Uzairu A, Shallangwa GA, Uba S (2020) In-silico activity prediction and docking studies of some 2, 9-disubstituted 8-phenylthio/phenylsulfinyl-9 h-purine derivatives as Anti-proliferative agents. *Heliyon* 6: e03158
14. Adeniji SE, Uba S, Uzairu A (2020) Multi-linear regression model, molecular binding interactions and ligand-based design of some prominent compounds against *M. tuberculosis*. *Network Model Anal Health Inform Bioinform* 9(8):1–18
15. Abdullahi M, Shallangwa GA, Uzairu A (2020) In silico QSAR and molecular docking simulation of some novel aryl sulfonamide derivatives as inhibitors of H5N1 influenza A virus subtype. *Beni-Suef Univ J Basic Appl Sci* 9(2):1–13

#### Publisher's Note

Springer Nature remains neutral with regard to jurisdictional claims in published maps and institutional affiliations.

**Submit your manuscript to a SpringerOpen<sup>®</sup> journal and benefit from:**

- Convenient online submission
- Rigorous peer review
- Open access: articles freely available online
- High visibility within the field
- Retaining the copyright to your article

Submit your next manuscript at ► [springeropen.com](https://www.springeropen.com)